BIOCHEMISTRY
including biophysical chemistry & molecular biology

Article

pubs.acs.org/biochemistry

Structural Consequences of Cysteinylation of Cu/Zn-Superoxide Dismutase

Jared R. Auclair,[†,‡] Heather R. Brodkin,[†,§] J. Alejandro D'Aquino,[†] Gregory A. Petsko,[†] Dagmar Ringe,[†] and Jeffrey N. Agar*[,†,‡]

[†]Departments of Biochemistry and Chemistry and Rosenstiel Basic Medical Sciences Research Center, Brandeis University, Waltham, Massachusetts 02454, United States

Supporting Information

ABSTRACT: The metalloenzyme Cu/Zn-superoxide dismutase (SOD1) catalyzes the reduction of superoxide anions into molecular oxygen and hydrogen peroxide. Hydrogen peroxide can oxidize SOD1, resulting in aberrant protein conformational changes, disruption of SOD1 function, and DNA damage. Cells may have evolved mechanisms of regulation that prevent such oxidation. We observed that cysteinylation of cysteine 111 (Cys_{111}) of SOD1 prevents oxidation by peroxide (DOI 10.1021/bi4006122). In this article, we characterize cysteinylated SOD1 using differential scanning fluorometry and X-ray crystallography. The stoichiometry of binding was one cysteine per SOD1 dimer, and there does not appear to be free volume for a second cysteine without disrupting the dimer interface. Much of the three-dimensional structure of SOD1 is unaffected by cysteinylation. However, local conformational changes are observed in the cysteinylated monomer that include changes in conformation of the electrostatic loop (loop VII; residues 133−144) and the dimer interface (loop VI; residues 102−115). In addition, our data shows how cysteinylation precludes oxidation of cysteine 111 and suggests possible cross-talk between the dimer interface and the electrostatic loop.

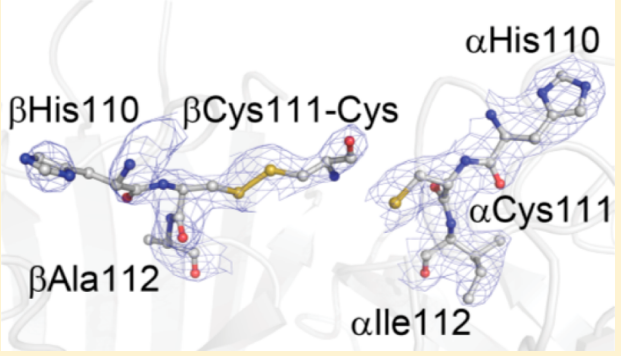

INTRODUCTION

Cu/Zn-superoxide dismutase (SOD1) is a 153 amino acid homodimer that catalyzes the metal-dependent reduction of superoxide anions ($O_2^{\bullet-}$) to hydrogen peroxide (H_2O_2) and oxygen (O_2).[1] One of the products of the reaction, hydrogen peroxide, can damage the enzyme; it oxidizes Cys_{111} first and then Trp32 and the active site histides, leading to inactivation of SOD1.[2,3] This activity-dependent inactivation leads to an increase in superoxide anions, which in turn produces negative effects such as aberrant protein conformational changes, disruption of enzyme function, mutation of DNA, and so on.[4−6] In a sister manuscript (DOI 10.1021/bi4006122), we demonstrate cysteinylation of Cys_{111} and show that cysteinylation prevents oxidation of SOD1 in vitro. This post-translational modification raises the possibility that cysteinylation is part of a regulatory mechanism that protects SOD1 from oxidation by its product, hydrogen peroxide.

Cysteinylation is a post-translational modification that remains largely uncharacterized because protein preparations are generally treated with disulfide reducing agents such as dithiothreitol (DTT), 2-mercaptoethanol (*β*-Me), or *tris*(2-carboxyethyl)phosphine (TCEP), which remove cysteinlyation. Despite this, cysteinylation has been observed, but not well characterized, in transthyretin (TTR), human serum albumin, and the k1 light chain from an amyloid patient.[7,8] Cysteinylation has also been observed during oxidative stress treatment of *Bacillus subtilis* strains, where it may protect cysteine residues from oxidation.[9]

To better understand SOD1 cysteinlyation, we set out to characterize its structure using differential scanning fluorometry and X-ray crystallography. We present the first structural analysis of cysteinylated SOD1, and to the best of our knowledge of any cysteinylated protein.

METHODS

Protein Expression and Purification. The construct for expression of human SOD1 (hSOD1) in *S. cerevisiae* was obtained through the generous gift of Dr. P. John Hart, Ph.D. (University of Texas Health Science Center, San Antonio). Expression and purification was carried out as previously published.[10,11] Briefly, hSOD1 in the yeast expression vector YEp-351 was transformed into EGy118ΔSOD1 yeast and grown at 30 °C for approximately 48 h. Cultures were pelleted, lysed using 0.5 mm glass beads and a blender, and subjected to a 60% ammonium sulfate cut. After ammonium sulfate precipitation, the sample was pelleted and the supernatant was diluted with 0.19 volumes of a low salt buffer (50 mM sodium phosphate, 150 mM sodium chloride, 0.1 M EDTA,

Received: May 15, 2013
Revised: July 30, 2013
Published: August 6, 2013

0.25 mM DTT, pH 7.0) to a final concentration of 2.0 M ammonium sulfate. This sample was then purified using a Phenyl Sepherose 6 Fast Flow (High Sub) hydrophobic interaction chromatography column (GE Life Sciences) using a 300 mL linearly decreasing salt gradient from a high salt buffer (2.0 M ammonium sulfate, 50 mM sodium phosphate, 150 mM sodium chloride, 0.1 M EDTA, 0.25 mM DTT, pH 7.0) to the low salt buffer. Samples containing SOD1 were eluted between 1.6 and 1.1 M ammonium sulfate, pooled, and buffer exchanged to a 10 mM Tris, pH 8.0, buffer. The protein was then loaded onto a Mono Q 10/100 anion exchange chromatography column (GE Life Sciences) and eluted using a 200 mL linearly increasing salt gradient from a low salt buffer (10 mM Tris, pH 8.0) to a high salt buffer (10 mM Tris, pH 8.0, 1 M sodium chloride). The gradient was run from 0 to 30% 10 mM Tris, pH 8.0, 1 M sodium chloride, and SOD1 eluted between 5 and 12% 10 mM Tris, pH 8.0, 1 M sodium chloride. SOD1 protein was diluted into 50% acetonitrile and 0.1% formic acid (MALDI) or 5% acetonitrile and 0.1% formic acid (FTMS), confirmed via MALDI-TOF and FTMS analysis, and quantified using the Bradford assay with yields of 6 mg/8 L (0.75 mg/L). In addition, the majority of SOD1 samples are fully metalated as determined by intact mass analysis using a Fourier transform mass spectrometer, which is in agreement with previous ICP-MS analysis we performed on a representative sample.[12]

Crystallization, Data Collection, and Refinement. Crystals of cysteinylated SOD1 were grown using the hanging drop method at 25 °C. SOD1 was cysteinylated by incubating an 8 mg/mL stock solution of protein with a 40-fold molar excess of cysteine (20.7 mM) for 30−60 min prior to setting the drop. Four microliter drops were formed by mixing equal volumes of cysteinylated protein and a crystallization solution containing 0.1 M MES, pH 6.25, and 20% PEG 3350. After 1−3 weeks, crystals suitable for X-ray crystallography appeared in the drops. The crystals were harvested directly from the drops, transferred to a solution of 0.1 M MES, pH 6.25, with 20% PEG 3350 containing 20% glycerol as a cryoprotectant, and subsequently flash frozen in liquid nitrogen prior to data collection.

Data were collected at beamline 23-ID-B at GM/CA-CAT (Advanced Photon Source (APS), Argonne National Laboratory (ANL), Argonne, IL) at 100 K using a MarMosaic CCD detector. Diffraction images were integrated and scaled using HKL2000.[13] The integrated and scaled file from HKL2000 was used to assess the quality of the data and to rule out the possibility of twinning. We also exploited the graphics provided by the twinning server[14] to visualize how our data compared to twinned data (Supporting Information Figure S1). The crystals have the symmetry of space group $P6_3$ with unit cell dimensions $a = b = 113.1$ Å, $c = 70.6$ Å, $\alpha = \beta = 90°$, and $\gamma = 120°$. The structure was solved by molecular replacement using PHENIX AutoMR,[15] and the coordinates of wild-type human SOD1 (PDB entry 1SPD[16]) were used as a starting model. The diffraction anisotropy server at the Molecular Biology Institute at UCLA (http://services.mbi.ucla.edu/anisoscale) was used to correct for anisotropy.[17]

In order to model the cysteine modification, a PDB file with cysteine only was created, opened in Coot,[18] and then modeled into the appropriate density and merged with the existing PDB. After a round of simulated annealing, multiple cycles of iterative manual building were performed in Coot[18] and refined against an amplitude-based maximum-likelihood target function in PHENIX until the R_{free} could no longer be reduced. In addition, anisotropic refinements (18 TLS groups selected by PHENIX), water picking with PHENIX, and group *B*-factors were used in refinement. The atomic coordinates of cysteinylated SOD1 have been deposited in the Protein Data Bank (PDB 4FF9).

Differential Scanning Fluorometry (DSF). The melting temperature of SOD1 was monitored using differential scanning fluorometry in the presence or absence of cysteine and hydrogen peroxide. In the first sequence of reactions, 20 μM SOD1 was incubated with a 40-fold molar excess of cysteine (800 μM) and 20X SYPRO Orange, and the mixture was added to a 96-well plate. In the second sequence of reactions, 20 μM SOD1 was incubated with 500-fold molar excess of hydrogen peroxide (10 mM) and 20X SYPRO Orange, and the mixture was added to a 96-well plate. Reactions were diluted 1:1 (10 μM SOD1 final concentration) prior to analysis. The melting temperature of the protein was monitored using an RT-PCR machine (Applied Biosystems) with a 0.3 °C increase in temperature every minute from 25 to 100 °C. Data were analyzed by subtracting a blank without protein from each respective well, normalized to one, and the temperature versus relative fluorescence was plotted.[19] Reactions were repeated in triplicate.

RESULTS

Monocysteinylated SOD1. Following in vitro cysteinylation, mass spectrometry studies showed a mixture of unmodified and cysteinylated SOD1 monomer. Because the mass spectrometry methods dissociate the labile SOD1 dimer before detection, they could not conclusively differentiate between there being monocysteinylated SOD1 dimer or a mixture of dicysteinlated SOD1 dimer (each Cys_{111} residue modified) and unmodified dimer. The X-ray crystal structure of SOD1-Cys was consistent with a binding stoichiometry of one cysteine attached to a single Cys_{111} of the SOD1 dimer (Figure 1). There does not appear to be free volume for a second cysteine to modify the related Cys_{111} on the opposite subunit without disrupting the dimer interface.

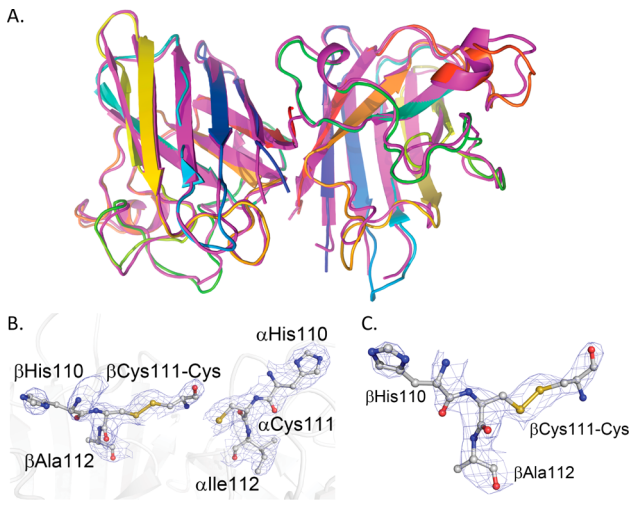

Figure 1. Cysteinlyation of Cys_{111} in SOD1. (A) Structure of cysteinlyated SOD1 dimer (magenta) superimposed with wild-type SOD1 (PDB ID: 1SPD[16]). The global structure is conserved in the cysteinlyated SOD1. (B) Cysteinylation is observed only on chain β. (C) Zoom in of the cysteinlyated Cys_{111} with electron density contoured at 1σ.

dx.doi.org/10.1021/bi400613h | *Biochemistry* 2013, 52, 6145−6150

Cysteinylation of Cys_{111} Perturbs the Local Structure of the Dimer Interface (Loop VI) and the Electrostatic Loop (Loop VII). We solved the crystal structure of SOD1-Cys to 2.5 Å resolution after screening over 40 different crystals using different crystallization and cryo-preservation conditions (Supporting Information Table 1). Only one condition revealed cysteinylation on one monomer. The global structure of cysteinlyated SOD1 was similar to that of other structures for this enzyme deposited in the PDB (Figure 1A). Superimposing the coordinates of wild-type SOD1 (PDB ID: 1SPD) and SOD1-Cys (this work) yields an rms deviation of 1.0 Å over 153 α atoms for the α chain and 1.0 Å for 151 α atoms for the β chain. The refined model contains 1 homodimer in the asymmetric unit, 2 copper ions and 2 zinc ions (fully occupied), 1 cysteine modification on the β chain, and 24 waters. Details of the structure determination and refinement parameters are listed in Table 1. In addition, the protein exhibits good geometry, where 88.7% of the residues are in the most favored region of the Ramachandran analysis, 8.9% are in the allowed regions, and 2.4% are outliers (7 total). Of those outliers, two were at the N-terminus, two were at the dimer interface, and two were in loops. There was missing density for the side chains of residues 3, 23, 24, and 36 on the α chain and 30, 36, 70, 100, and 112 on the β chain, so those residues were modeled as alanine. In addition, no electron density was observed for residues 24 and 25 in loop II of the β chain; thus, they were deleted from the model and not included in the final structure.

Table 1. Crystallographic Data and Refinement Statistics

Data Collection Statistics	SOD1-Cys
beamline	APS, GM/CA-CAT, ID-B
wavelength	0.95 Å
space group	$P6_3$
cell constants	a = 113.1 Å
	b = 113.1 Å
	c = 70.6 Å
	$\alpha = \beta$ = 90°
	γ = 120°
total reflections	16 978
unique reflections	15 290
resolution limit (Å)	2.48 (2.48−2.57)[a]
completeness (%)	94.8 (100.0)
redundancy	10.9 (10.7)
$I/\sigma I$	25.6 (4.8)
R_{merge} (%)	0.083 (0.56)
Refinement Statistics	**SOD1-Cys**
resolution range (Å)	2.48−27.15
R_{free} test set size	1688
R_{work} (%)	27.6
R_{free} (%)	33.5
no. of atoms	
total	2221
protein	2193
water	24
copper	2
zinc	2
B-factors (overall)	52.13
rms deviations	
bond lengths (Å)	0.009
bond angles (deg)	1.3

[a]Parentheses are for statistics in the highest resolution shell.

Superimposing wild-type SOD1 (PDB ID: 1SPD[16]) and SOD1-Cys show some differences in two loop regions (loop VI, Figure 2A,B; loop VII, Figure 2C,D) of SOD1. Interestingly,

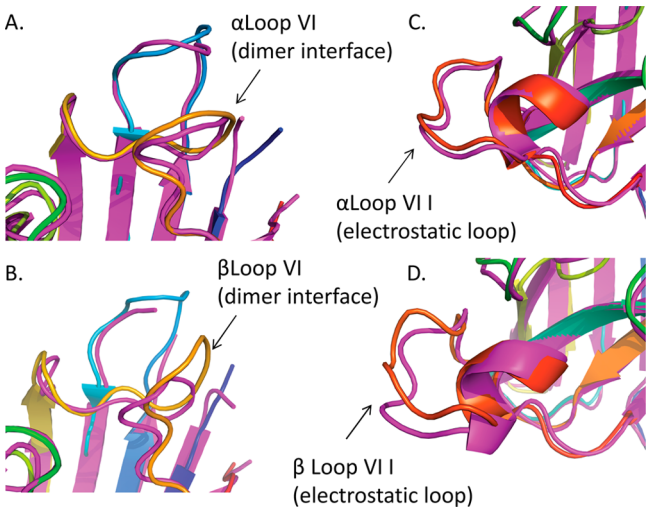

Figure 2. Cysteinlyation causing local structural changes in SOD1. The structure of cysteinlyated SOD1 dimer (magenta) is superimposed with wild-type SOD1 (PDB ID: 1SPD[16]). The Cys_{111}-Cys loop VI (magenta) is overlaid with 1SPD,[16] showing small changes in the region where (A) no cysteinylation is observed and (B) large, local structural changes are observed at the site of the modification on chain β. (C) The electrostatic loop of the unmodified monomer is similar to SOD1 (PDB ID: 1SPD), whereas (D) the electrostatic loop of the modified monomer undergoes a conformational change.

the unmodified monomer (chain α) has similar structure at the dimer interface (particularly loop VI, containing Cys_{111}) compared to that of the starting model (PDB ID: 1SPD); however, the modified (cysteinylated) monomer (chain β) shows local perturbations of the dimer interface. This is evidenced by a 3.6 Å shift in loop VI between the Cα of Gly_{108} in SOD1-Cys compared to that of the model structure (PDB ID: 1SPD) (Figure 2A compared to Figure 2B). In addition to the dimer interface, the cysteinylated monomer (chain β) also appears to have a local conformational change at the electrostatic loop (loop VII) as evidenced by a 3.4 Å shift between the Cα of Gly_{130} in SOD1-Cys compared to that of the model structure (Figure 2C compared to Figure 2D).

Oxidation Destabilized SOD1. Differential scanning fluorometry (DSF) was used to measure the thermal stability of SOD1, oxidized SOD1 (SOD1-ox), and SOD1-Cys. The fluorescence signal was monitored as native, oxidized, and cysteinylated SOD1 samples were heated in the presence of a fluorescent dye. Oxidation decreased the melting temperature (T_m) of SOD1 approximately 23 °C, whereas cysteinylation decreased the melting temperature approximately 5 °C (Figure 3), thus suggesting oxidation had a profound effect on SOD1 stability compared to that of unmodified and cysteinylated SOD1.

DISCUSSION

Here, we present a structural analysis of SOD1 modified by cysteine (cysteinylated). The crystal structure suggests that the global structure of SOD1 is conserved upon modification. The

dx.doi.org/10.1021/bi400613h | Biochemistry 2013, 52, 6145−6150

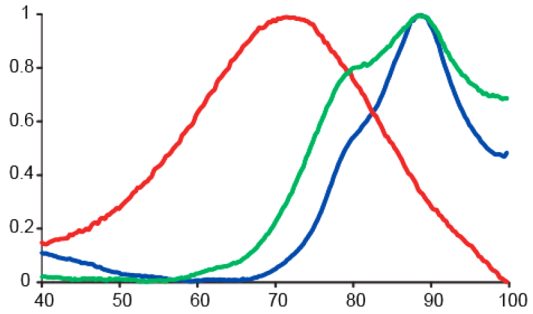

Figure 3. Oxidation and cysteinylation destabilizing SOD1. Differential scanning fluorometry was used to measure the melting temperature of SOD1, peroxide-oxidized SOD1, and SOD1-Cys. Melting temperature curves of SOD1 (blue), peroxide oxidized SOD1 (red), and cysteinlyated SOD1 (green). Oxidation destabilized SOD1 by approximately 23 °C, whereas cysteinylation destabilized SOD1 by approximately 5 °C. Folding–unfolding transitions (thermal denaturation curves) were measured in triplicate.

2.5 Å SOD1-Cys crystal structure suggests that Cys_{111} is the site of modification and that only one cysteine modification per dimer occurs because of steric restriction of the symmetry-related site when the first one is modified. Local conformational changes were observed at the site of the modification in the dimer interface (loop VI) and at the distal electrostatic loop (loop VII) of the modified monomer (chain β); these conformational changes were not observed in the unmodified monomer (chain α) and are thus not likely because of crystal packing. In addition, these conformation changes are consistent with allosteric cross-talk between loop VI and loop VII. Modification of the electrostatic loop is interesting, considering the fact that was the one common effect of 13 ALS-causing mutations and the site for the gain-of-interaction found in crystal structures of fALS SOD1 variants by Elam et al.[20,21]

Because of an *R*-value of 27.6% and an R_{free} of 33.5%, we used phenix.xtriage to assess the quality of the data and to rule out the possibility of twinning. We also exploited the graphics provided by the twinning server[14] to visualize how our data compared to twinned data (Supporting Information Figure S1). The results of both twinning analyses showed that our data set was untwinned. After further inspection of the data, it became evident that the raw data showed severe anisotropy and required a correction. Because the anisotropy lowers the resolution in one dimension of the frame, we expected our *R*-values to be somewhat higher as a result. We believe that an *R*-value of 27.6% and an R_{free} value of 33.5% are consistent with the anisotropic nature of the data set. Furthermore, the difference between *R*-value and R_{free} do not show evidence of over-refinement. Finally, the crystal represents a mixture of modified and unmodified enzyme; in view of the conformational changes throughout the molecule produced by the modification (and only observed in the modified chain), that would mean any single mode cannot adequately account for all the scattering.

SOD1, SOD1-ox, and SOD1-Cys stability was monitored using DSF and showed a 23 °C decrease in SOD1 melting temperature upon oxidation and only a 5 °C decrease in melting temperature upon cysteinylation. This suggests oxidation causes a profound destabilization of SOD1 compared to unmodified and cysteinylated SOD1. Therefore, cysteinlyation only causes a small destabilization and, as we have shown previously, can potentially abrogate the large destabilization due to oxidation (DOI 10.1021/bi4006122). The small conformational changes in the electrostatic loop and dimer interface may be linked to SOD1-Cys stability.

Interestingly, 2-mercaptoethanol-modified (2-ME) SOD1 has been described previously and its crystal structure has been solved[22,23] (PDB ID: 3T5W[23]). The smaller 2-ME was able to modify both Cys_{111} residues of the SOD1 dimer, change the electrostatic loop, and stabilize SOD1.[22] This is in comparison to monocysteinylation, which changed the electrostatic loop but resulted in a small destabilization. Thus, 2-ME SOD1 and monocysteinylated SOD1 share a similar structure, including the electrostatic loop, with the exception of changes observed in the residues immediately preceding cysteinylated Cys_{111} (residues 108–111).[23] These data suggest that loop VI, in particular residues 108–111, and the electrostatic loop, may play a role in SOD1 stability.

SOD1 can be oxidized by one of its reaction products, hydrogen peroxide, which can cause protein conformational change and enzyme inactivation[4−6] and promote proteolytic degradation.[24,25] Thus, it is possible that some sort of regulation (or protection) is present in the cell. We have previously observed cysteinlyation of SOD1 in nervous tissue and seen that cysteinylation protects against oxidation in vitro, suggesting cysteinylation could play a protective role for SOD1 under conditions of oxidative stress. The data presented here suggest a structural mechanism where cysteinylation can prevent oxidation of the modified cysteine in the dimer interface, whereas oxidation of the unmodified cysteine in the dimer interface can still occur. However, oxidation of just one cysteine at the dimer interface would not cause the electrostatic repulsion, and consequent dimer disruption, that would occur if both symmetry-related Cys_{111} residues, which are only 7 Å apart, acquired permanent negative charges via oxidation.

Post-translational modifications of SOD1, including oxidation of Cys_{111}, have been implicated in ALS, Parkinson's, and Alzheimer's diseases.[26−31] Having a mechanism to block oxidation of Cys_{111} could be advantageous in this sense as well. Further, both the electrostatic loop [32] and dimer dissociation[10,28,33,34] have been implicated in fALS, and our SOD1-Cys structure suggests that cysteinylation perturbs both of these regions. These local perturbations of SOD1 may prove to be crucial to the protein function and stability and provide a regulatory function in fALS.

Here, we present the structure of cysteinylated SOD1 and show that modification may prevent the negative effects of oxidation on SOD1 and thereby may function in a regulatory manner. In so doing, it may also prevent the deleterious effects oxidation may have on dimer stability, effects that have been postulated to lead to the SOD1-dependent form of ALS. Therapeutic strategies to mimic the effects of cysteinylation may represent a new approach to the prevention of this disease.

■ ASSOCIATED CONTENT

Ⓢ Supporting Information

Crystallization and cryopreservation conditions; twinning determination plot. This material is available free of charge via the Internet at http://pubs.acs.org.

■ AUTHOR INFORMATION

Corresponding Author

*J. N. Agar: e-mail, j.agar@neu.edu; phone, (617) 373-5909.

Present Addresses

[‡]Department of Chemistry and Chemical Biology and Pharmaceutical Sciences and the Barnett Institute, Northeastern University, Boston, Massachusetts 02115, United States.
[§]Alkermes, Waltham, Massachusetts 02451, United States.

Funding

This work was supported in part by grants from National Institutes of Health (1R01NS065263-01 and 1R21NS071256 to J.N.A.) and Fidelity Biosciences Research Initiative to G.A.P. and D.R.

Notes

The authors declare no competing financial interest.

■ ACKNOWLEDGMENTS

Use of the Advanced Photon Source, an Office of Science User Facility operated for the U.S. Department of Energy (DOE) Office of Science by Argonne National Laboratory, was supported by the U.S. DOE under contract DE-AC02-06CH11357. We thank Dr. P. John Hart for the generous gift of the YEP351-SOD1 plasmid and EGy118-(ΔSOD1) yeast cells used to express SOD1 in this study. We also thank members of the Agar and Petsko/Ringe Laboratories for thoughtful discussions, insights, and critically reviewing this manuscript.

■ REFERENCES

(1) McCord, J. M., and Fridovich, I. (1968) The reduction of cytochrome c by milk xanthine oxidase. *J. Biol. Chem 243*, 5753−5760.

(2) Karunakaran, C., Zhang, H., Crow, J. P., Antholine, W. E., and Kalyanaraman, B. (2004) Direct Probing of Copper Active Site and Free Radical Formed during Bicarbonate-dependent Peroxidase Activity of Bovine and Human Copper,Zinc-superoxide Dismutases: Low-Temperature Electron Paramagnetic Resonance and Electron Nuclear Double Resonance Studies. *J. Biol. Chem. 279*, 32534−32540.

(3) Zhang, H., Andrekopoulos, C., Joseph, J., Chandran, K., Karoui, H., Crow, J. P., and Kalyanaraman, B. (2003) Bicarbonate-dependent peroxidase activity of human Cu,Zn-superoxide dismutase induces covalent aggregation of protein: intermediacy of tryptophan-derived oxidation products. *J. Biol. Chem. 278*, 24078−24089.

(4) Keithley, E. M., Canto, C., Zheng, Q. Y., Wang, X., Fischel-Ghodsian, N., and Johnson, K. R. (2005) Cu/Zn superoxide dismutase and age-related hearing loss. *Hear. Res. 209*, 76−85.

(5) Phillips, J. P., Tainer, J. A., Getzoff, E. D., Boulianne, G. L., Kirby, K., and Hilliker, A. J. (1995) Subunit-destabilizing mutations in Drosophila copper/zinc superoxide dismutase: neuropathology and a model of dimer dysequilibrium. *Proc. Natl. Acad. Sci. U. S. A. 92*, 8574−8578.

(6) Woodruff, R. C., Phillips, J. P., and Hilliker, A. J. (2004) Increased spontaneous DNA damage in Cu/Zn superoxide dismutase (SOD1) deficient Drosophila. *Genome 47*, 1029−1035.

(7) Kleinova, M., Belgacem, O., Pock, K., Rizzi, A., Buchacher, A., and Allmaier, G. (2005) Characterization of cysteinylation of pharmaceutical-grade human serum albumin by electrospray ionization mass spectrometry and low-energy collision-induced dissociation tandem mass spectrometry. *RCM 19*, 2965−2973.

(8) Lim, A., Wally, J., Walsh, M. T., Skinner, M., and Costello, C. E. (2001) Identification and location of a cysteinyl posttranslational modification in an amyloidogenic kappa1 light chain protein by electrospray ionization and matrix-assisted laser desorption/ionization mass spectrometry. *Anal. Biochem. 295*, 45−56.

(9) Hochgrafe, F., Mostertz, J., Pother, D. C., Becher, D., Helmann, J. D., and Hecker, M. (2007) S-cysteinylation is a general mechanism for thiol protection of Bacillus subtilis proteins after oxidative stress. *J. Biol. Chem. 282*, 25981−25985.

(10) Doucette, P. A., Whitson, L. J., Cao, X., Schirf, V., Demeler, B., Valentine, J. S., Hansen, J. C., and Hart, P. J. (2004) Dissociation of human copper-zinc superoxide dismutase dimers using chaotrope and reductant. Insights into the molecular basis for dimer stability. *J. Biol. Chem. 279*, 54558−54566.

(11) Hayward, L. J., Rodriguez, J. A., Kim, J. W., Tiwari, A., Goto, J. J., Cabelli, D. E., Valentine, J. S., and Brown, R. H., Jr. (2002) Decreased metallation and activity in subsets of mutant superoxide dismutases associated with familial amyotrophic lateral sclerosis. *J. Biol. Chem. 277*, 15923−15931.

(12) Auclair, J. R., Boggio, K. J., Petsko, G. A., Ringe, D., and Agar, J. N. (2010) Strategies for stabilizing superoxide dismutase (SOD1), the protein destabilized in the most common form of familial amyotrophic lateral sclerosis. *Proc. Natl. Acad. Sci. U. S. A. 107*, 21394−21399.

(13) Otwinowski, Z., and Minor, W. (1997) Processing of X-ray diffraction data collected in oscillation mode. *Methods Enzymol. 276*, 307−326.

(14) Padilla, J. E., and Yeates, T. O. (2003) A statistic for local intensity differences: robustness to anisotropy and pseudo-centering and utility for detecting twinning. *Acta Crystallogr., Sect. D: Biol. Crystallogr. 59*, 1124−1130.

(15) Adams, P. D., Grosse-Kunstleve, R. W., Hung, L. W., Ioerger, T. R., McCoy, A. J., Moriarty, N. W., Read, R. J., Sacchettini, J. C., Sauter, N. K., and Terwilliger, T. C. (2002) PHENIX: building new software for automated crystallographic structure determination. *Acta Crystallogr., Sect. D: Biol. Crystallogr. 58*, 1948−1954.

(16) Deng, H. X., Hentati, A., Tainer, J. A., Iqbal, Z., Cayabyab, A., Hung, W. Y., Getzoff, E. D., Hu, P., Herzfeldt, B., Roos, R. P., et al. (1993) Amyotrophic lateral sclerosis and structural defects in Cu,Zn superoxide dismutase. *Science 261*, 1047−1051.

(17) Strong, M., Sawaya, M. R., Wang, S. S., Phillips, M., Cascio, D., and Eisenberg, D. (2006) Toward the structural genomics of complexes: Crystal structure of a PE/PPE protein complex from Mycobacterium tuberculosis. *Proc. Natl. Acad. Sci. U. S. A. 103*, 8060−8065.

(18) Emsley, P., and Cowtan, K. (2004) Coot: model-building tools for molecular graphics. *Acta Crystallogr., Sect. D: Biol. Crystallogr. 60*, 2126−2132.

(19) Vedadi, M., Niesen, F. H., Allali-Hassani, A., Fedorov, O. Y., Finerty, P. J., Jr., Wasney, G. A., Yeung, R., Arrowsmith, C., Ball, L. J., Berglund, H., Hui, R., Marsden, B. D., Nordlund, P., Sundstrom, M., Weigelt, J., and Edwards, A. M. (2006) Chemical screening methods to identify ligands that promote protein stability, protein crystallization, and structure determination. *Proc. Natl. Acad. Sci. U. S. A. 103*, 15835−15840.

(20) Elam, J. S., Taylor, A. B., Strange, R., Antonyuk, S., Doucette, P. A., Rodriguez, J. A., Hasnain, S. S., Hayward, L. J., Valentine, J. S., Yeates, T. O., and Hart, P. J. (2003) Amyloid-like filaments and water-filled nanotubes formed by SOD1 mutant proteins linked to familial ALS. *Nat. Struct. Biol. 10*, 461−467.

(21) Taylor, D. M., Gibbs, B. F., Kabashi, E., Minotti, S., Durham, H. D., and Agar, J. N. (2007) Tryptophan 32 potentiates aggregation and cytotoxicity of a copper/zinc superoxide dismutase mutant associated with familial amyotrophic lateral sclerosis. *J. Biol. Chem. 282*, 16329−16335.

(22) Fujiwara, N., Nakano, M., Kato, S., Yoshihara, D., Ookawara, T., Eguchi, H., Taniguchi, N., and Suzuki, K. (2007) Oxidative modification to cysteine sulfonic acid of Cys111 in human copper-zinc superoxide dismutase. *J. Biol. Chem. 282*, 35933−35944.

(23) Ihara, K., Fujiwara, N., Yamaguchi, Y., Torigoe, H., Wakatsuki, S., Taniguchi, N., and Suzuki, K. (2012) Structural switching of Cu,Zn-superoxide dismutases at loop VI: Insights from the crystal structure of beta-mercaptoethanol modified enzyme. *Biosci. Rep. 32*, 539−548.

(24) Davies, K. J., and Goldberg, A. L. (1987) Proteins damaged by oxygen radicals are rapidly degraded in extracts of red blood cells. *J. Biol. Chem. 262*, 8227−8234.

(25) Davies, K. J., and Goldberg, A. L. (1987) Oxygen radicals stimulate intracellular proteolysis and lipid peroxidation by independent mechanisms in erythrocytes. *J. Biol. Chem. 262*, 8220−8226.

(26) Bredesen, D. E., Ellerby, L. M., Hart, P. J., Wiedau-Pazos, M., and Valentine, J. S. (1997) Do posttranslational modifications of

CuZnSOD lead to sporadic amyotrophic lateral sclerosis? *Ann. Neurol. 42*, 135−137.
(27) Kabashi, E., Valdmanis, P. N., Dion, P., and Rouleau, G. A. (2007) Oxidized/misfolded superoxide dismutase-1: the cause of all amyotrophic lateral sclerosis? *Ann. Neurol. 62*, 553−559.
(28) Rakhit, R., Crow, J. P., Lepock, J. R., Kondejewski, L. H., Cashman, N. R., and Chakrabartty, A. (2004) Monomeric Cu,Zn-superoxide dismutase is a common misfolding intermediate in the oxidation models of sporadic and familial amyotrophic lateral sclerosis. *J. Biol. Chem. 279*, 15499−15504.
(29) Rakhit, R., Cunningham, P., Furtos-Matei, A., Dahan, S., Qi, X. F., Crow, J. P., Cashman, N. R., Kondejewski, L. H., and Chakrabartty, A. (2002) Oxidation-induced misfolding and aggregation of superoxide dismutase and its implications for amyotrophic lateral sclerosis. *J. Biol. Chem. 277*, 47551−47556.
(30) Shibata, N., Hirano, A., Kobayashi, M., Sasaki, S., Kato, T., Matsumoto, S., Shiozawa, Z., Komori, T., Ikemoto, A., Umahara, T., et al. (1994) Cu/Zn superoxide dismutase-like immunoreactivity in Lewy body-like inclusions of sporadic amyotrophic lateral sclerosis. *Neurosci. Lett. 179*, 149−152.
(31) Choi, J., Rees, H. D., Weintraub, S. T., Levey, A. I., Chin, L. S., and Li, L. (2005) Oxidative modifications and aggregation of Cu,Zn-superoxide dismutase associated with Alzheimer and Parkinson diseases. *J. Biol. Chem. 280*, 11648−11655.
(32) Molnar, K. S., Karabacak, N. M., Johnson, J. L., Wang, Q., Tiwari, A., Hayward, L. J., Coales, S. J., Hamuro, Y., and Agar, J. N. (2009) A common property of amyotrophic lateral sclerosis-associated variants: destabilization of the copper/zinc superoxide dismutase electrostatic loop. *J. Biol. Chem. 284*, 30965−30973.
(33) Hornberg, A., Logan, D. T., Marklund, S. L., and Oliveberg, M. (2007) The coupling between disulphide status, metallation and dimer interface strength in Cu/Zn superoxide dismutase. *J. Mol. Biol. 365*, 333−342.
(34) Rakhit, R., Robertson, J., Vande Velde, C., Horne, P., Ruth, D. M., Griffin, J., Cleveland, D. W., Cashman, N. R., and Chakrabartty, A. (2007) An immunological epitope selective for pathological monomer-misfolded SOD1 in ALS. *Nat. Med. 13*, 754−759.